Granulocyte–endothelium initial adhesion

Analysis of transient binding events mediated by E-selectin in a laminar shear flow

Gilles Kaplanski,* Catherine Farnarier,* Olivier Tissot,* Anne Pierres,* Anne-Marie Benoliel,* Marie-Christine Alessi,‡ Solange Kaplanski,* and Pierre Bongrand*

*Laboratoire d'Immunologie, Hôpital de Sainte-Marguerite, BP29, 13277 Marseille Cedex 09; and ‡Laboratoire d'Hématologie, CHU Timone, 13005 Marseille, France

ABSTRACT The adhesion of moving cells to receptor-bearing surfaces is a key step to many important biological processes. Attachment was subjected to extensive modeling. However, the numerical values of kinetic bonding parameters relevant to realistic models of cell adhesion remain poorly known. In this report, we describe the motion of human granulocytes to interleukin-1–activated endothelial cells in presence of a low hydrodynamic drag (a few piconewtons) estimated to be much weaker than a standard ligand–receptor bond. It was thus expected to visualize the formation and rupture of individual bonds. We observed multiple short-time cell arrests with a median duration of 2.43 s. Stop frequency, not duration, was significantly inhibited by anti-E-selectin antibodies. Binding efficiency exhibited an almost linear relationship with the inverse of cell velocity. The distribution of arrest duration was determined: results were consistent with the view that these arrests reflected the formation/dissociation of single ligand–receptor bonds with a spontaneous dissociation rate of 0.5 s^{-1}. The rate of bond formation was on the order of 0.04 s^{-1} when cells were freely rolling (mean velocity: 19 μm/s) and it exhibited an ~10-fold increase after the formation of a first adhesion.

INTRODUCTION

The adhesion of moving cells to other cells or surfaces is likely to play a critical role in many important biological processes such as lymphocyte-mediated cytotoxicity (1), phagocytosis (2), cancer cell metastasis (3), or tissue invasion by infectious microorganisms (4). An important example is the adhesion of blood granulocytes to endothelium as an early step of inflammation and immune defense (5).

During the last few years, much effort was done to characterize the molecules involved in neutrophil adhesion to blood vessels, leading to the following scheme: the generation of inflammatory cytokines in infected sites will induce the expression of adhesion molecules on endothelial cells (6); among these, E-selectin and P-selectin are long and flexible structures (7) with a peculiar ability to stick to carbohydrate sites borne by leukocytes moving with a velocity as high as several tens or hundreds of micrometers per second in flowing blood (8, 9). This binding will reduce cell velocity to a few micrometers per second. This slow motion, usually referred to as leukocyte rolling, allows the formation of additional bonds between β2-integrins expressed on granulocytes and intercellular adhesion molecules (ICAMs) constitutively present on endothelial cells (7, 9). This will lead to complete leukocyte arrest and subsequent transmigration toward peripheral tissues. Integrin-mediated adhesion requires a suitable activation of leukocytes by mediators, such as platelet-activating factor or interleukin 8, that may be secreted or expressed by endothelial cells (10–12).

Adhesive efficiency is clearly dependent on numerous parameters such as the wall shear rate, the area of cell-to-endothelium contact, density, mobility and affinity of ligand molecules, and presence of potentially repulsive elements present in the endothelium or leukocyte glycocalix (13–16). There is thus a need for quantitative models allowing both integration of experimental data and prediction of the outcome of cell–cell contact in various circumstances. A seminal model was built by Bell (17), who applied standard kinetic theory to the formation and dissociation of intercellular bonds. He emphasized the difference between kinetic constants for reactions occurring in fluid phase and on membrane surfaces: indeed, the latter may be lower by as much as four orders of magnitude. Further, Bell elaborated on a report by Zurkhov (18) on material resistance to account for the effect of stress on affinity constants. He suggested that the dissociation rate of stressed ligand–receptor bonds might be written as

$$k_- = k_{o-} \exp(\tau F/kTN), \qquad (1)$$

where k_- and k_{o-} are the stressed and unstressed dissociation constants, F is the applied force, k is Boltzmann's constant, T is the absolute temperature, N is the number of bonds resisting the disruptive force, and τ is a constant that was estimated at 0.5 nm.

Hammer and Lauffenburger (19) built on this approach and elaborated a dynamical model to determine whether cells would adhere to ligand-coated surfaces in conditions of flow. However, surface deformations were neglected. In a later work, Dembo et al. (20) studied the rate of peeling of a deformable one-dimensional membrane. They extended Eq. 1 by noticing that both association and dissociation constants might be affected by strain, and whereas the ratio k_+/k_- was expected to be decreased by a disruptive force, the rate of bond dissociation might be either increased (slip bonds) or decreased (catch bonds) by strain.

Address correspondence to P. Bongrand.

0006-3495/93/06/1922/12 $2.00

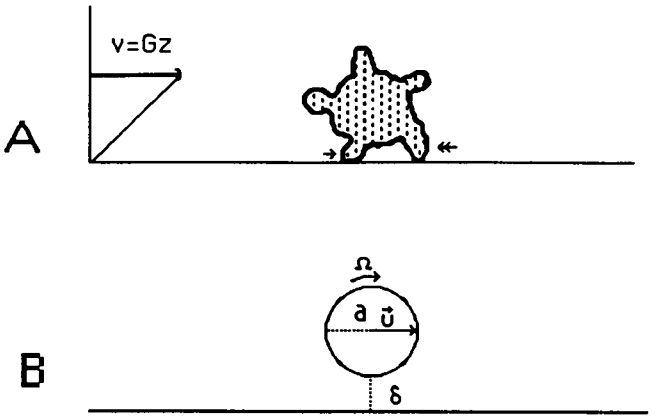

FIGURE 1 Model for cell rolling and adhesion. Cells were subjected to a laminar shear flow with velocity gradient G. (*A*) A bound cell is shown with adhesion at the tip of a protrusion (*arrow*). The adhesion is subjected to a disruption force including a tangential component F and a vertical component on the order of the product between hydrodynamic torque and cell radius. This will favor the formation of new bonds involving protrusions located at the front edge of the cell (*double arrow*). (*B*) To use Goldman's model, cells are viewed as smooth spheres separated from the substratum by a gap of width δ. a is the cell radius, U the cell translational velocity, and Ω its angular velocity.

More recently, Cozens-Roberts et al. (21) emphasized the limits of previous deterministic models in situations where cells might be bound by a few molecules. They provided a probabilistic model that yielded different predictions concerning the time required for cell attachment and detachment. The probabilistic approach was further used by Hammer and Apte (22), who performed extensive simulations of the movement of protrusion-coated cells moving near a flat surface in a shear flow. They were thus able to reproduce many patterns of leukocyte–endothelium interaction. Finally, Tözeren and Ley (23) showed that the rolling phenomenon might be critically dependent on the molecular properties of selectin–ligand association. See reference 24 for an illuminating review on models of receptor-mediated cell adhesion.

The problem with aforementioned approaches is that, although they rely on a broad amount of experimental data and thorough physical and biological reasoning, they make use of many unknown parameters that may critically influence the outcome of cell contact, particularly the rate of bond formation and dissociation. It is therefore useful to estimate the numerical values of these parameters in realistic models.

In this report, we study the detailed kinetics of bond formation and dissociation between activated neutrophils and endothelial cells interacting in a flow chamber. The basic idea was to use a very low flow rate, in order that the drag force exerted on individual cells be much lower than the mechanical strength of a single molecular bond. This approach should in principle allow direct visualization of bond formation and rupture. We observed frequent cell arrests of varying duration. These arrests were substantially inhibited by anti-E-selectin monoclonal antibodies, suggesting that they involved well-defined selectin–ligand interactions. The distribution of arrest duration was very accurately fitted by a quantitative model, strongly suggesting that these arrests reflected the formation of single molecular bonds, and allowing quantitative determination of the rate of bond formation and dissociation.

MODEL AND ASSUMPTIONS

Movement of free cells near a plane surface in laminar shear flow

Cells may be viewed as spheres coated with rigid protrusions, the tips of which are involved in contact formation (13, 22, 23). Following most aforementioned reports, the motion of free cells may be modeled within the framework of a theory elaborated by Goldman et al. (25) to describe the displacement of a neutrally buoyant sphere of radius a, separated from a flat surface by a gap of width δ in a laminar shear flow of shear rate (or velocity gradient) G (Fig. 1; see Table 1 for a complete list of symbols). Cells exhibit both translation (with velocity U parallel to the surface) and rotation (with angular velocity Ω). The relevance of Goldman's theory to actual cells was recently subjected to experimental check (26) using lymphoid cells moving along a nonadhesive surface. The experimental values of the dimensionless parameters U/aG and Ω were

$$U/aG = 0.86 \quad (2)$$

$$\Omega/G = 0.59. \quad (3)$$

The calculated value of δ was on the order of 0.5–2 μm, corresponding to the length of microvilli, as checked

TABLE 1 **Symbols**

a	Sphere radius
D	Diffusion coefficient
f	Friction coefficient
F	Hydrodynamic dragging force
k	Boltzmann's constant
k_-	Rate of bond dissociation
k_+	Rate of bond formation
L	Length of cell path
n	Number of cell stops
N	Number of bonds
p	Adhesion efficiency (μm^{-1})
P	Probability
$P_k(t)$	Probability for a cell to be attached by k bonds at time t after initial arrest
T	Absolute temperature
U	Cell translational velocity
Γ	Hydrodynamic torque exerted on a bound cell
δ	Width of cell-substratum gap
μ	Medium viscosity
ρ	Medium density
τ	Empirical parameter used to describe the effect of stress on bond lifetime
Ω	Cell angular velocity

with electron microscopy. Since U and Ω are expected to display moderate variations when δ is changed within reasonable limits (e.g., between $a/5$ and $a/500$), the aforementioned estimates may probably be considered as convenient orders of magnitude in many experimental situations.

Bond formation and arrest

It is important to know how many bonds are required to stop a cell. Recent experimental evidence (27, 28) confirmed previous theoretical estimates (17) and supported the view that the strength of many biologically relevant receptor–ligand bonds ranges between 10 and 40 pN. Furthermore, according to Goldman's theory, a substrate-bound cell exposed to a laminar flow experiences a drag force F and torque Γ given by

$$F = 32.05\mu a^2 G \quad (4)$$

$$\Gamma = 11.86\mu a^3 G, \quad (5)$$

where μ is the medium viscosity (i.e., 0.001 Pa·s in water), a is the sphere radius, and G is the wall shear rate (per second). The basis of our experimental approach was to use a low enough G value that bonds be subjected to minimal strain, thus allowing safe neglect of parameter τ defined by Eq. 1. Indeed, using blood granulocytes of 4.0-μm radius (mean radius was 4.0 ± 0.5 SE on a sample of 42 cells) and $G = 5.25/\text{s}$, the tangential force F and vertical force (i.e., ca. Γ/a) exerted on a single contact were 2.7 and 1.9, pN respectively (see Fig. 1). These values are ≥10-fold lower than the expected strength of molecular bonds. Also, it may be readily shown that Reynolds' number $a^2G\rho/\mu$, where ρ is the medium density, is much lower than unity. This shows that inertial effects are negligible. Bond formation can thus induce instantaneous cell arrest, in accordance with previous experimental results (29).

Expected behavior of substrate-bound cells

A convenient order of magnitude for the velocity U_b of a leukocyte bound to an endothelial cell by a single molecular bond may be estimated by equating the shear force to the viscous drag experienced by a receptor molecule embedded in the endothelial cell membrane (see Fig. 1):

$$fU_b = F, \quad (6)$$

where f is the friction coefficient. According to Einstein's relationship, f is equal to kT/D, where k is Boltzmann's constant, T is the absolute temperature, and D is the diffusion coefficient of a ligand molecule. D is expected to range between 0 (if the receptor is bound to cytoskeletal elements) and ca. 10^{-14} m^2/s (16). The maximum translation value of a cell of 4 μm radius bound by a single molecule is thus

$$U_b f = 32.054\,DaG/kT = 0.31G. \quad (7)$$

This is about one third of the expected velocity of free cells (Eq. 2).

Mean duration of cell attachment

A probabilistic model is required to deal with attachments mediated with a few molecular bonds. Therefore, we follow the approach described by Cozens-Roberts et al. (21) by considering the probability $P_i(t)$ that a cell be bound by i bonds at time t after the formation of a first bond. We use two phenomenological parameters, namely, bond formation probability k_+ and bond dissociation rate k_-. Following reference 21, we may write:

$$dP_1/dt = 2k_-P_2 - (k_+ + k_-)P_1 \quad (8)$$

$$dP_i/dt = k_+P_{i-1} + (i+1)k_-P_{i+1} - (k_+ + ik_-)P_i \quad \text{if } i > 1. \quad (9)$$

The four terms on the right side of Eq. 9 represent, respectively, the formation of a ith bond, dissociation of a bond in a contact with $i+1$ bonds, formation of a $(i+1)$th bond, and bond dissociation in a contact with i bonds. Eqs. 8 and 9 may be written in dimensionless form, using $1/k_-$ as a time unit. They were solved numerically using different values for the ratio k_+/k_- by step-by-step adjustment of parameters $P_1, P_2, \ldots P_{10}$ up to values of t low enough that the probability of having >10 bonds remain negligible. At time zero, all parameters P_i are zero except P_1, which is equal to 1. At any time, the sum of parameters P_i represents the probability that the cell remains bound. Numerical examples are shown on Fig. 2 *A*. It is clear that the ratio k_+/k_- may be readily derived from the ration t_{50}/t_{30} between the times when 50 and 30% of cells became detached from the substrate (Fig. 2 *B*). This finding was used to interpret experimental data.

MATERIALS AND METHODS

Cells

Human umbilical vein endothelial cells (HUVEC) were obtained by collagenase digestion (30). Umbilical veins were perfused with Hank's solution containing 0.3 U/ml collagenase A (Boehringer Mannheim GmBH, Mannheim, Germany). After 15 min at 37°C, they were gently massaged before perfusion with Hank's solution supplemented with 20% fetal calf serum (Gibco, Glasgow, Scotland). Cells were then washed and incubated in 25-ml Falcon culture vials (Becton & Dickinson France, Grenoble) that had been pretreated overnight with 1% gelatin (Sigma France, La Verpillière, France). Cells from one umbilical cord were added to each vial in 5 ml of 199 medium (Flow, Puteaux, France) supplemented with 15 mM Hepes buffer, 15 mM bicarbonate, 2 mM L-glutamine, 150 U/ml penicillin, 50 μg/ml streptomycin, and 20% fetal calf serum. When monolayers were confluent, cells were washed with cation-free Dulbecco's solution, then detached by a few minutes' exposure to 0.1% trypsin at 37°C and washed with 199 medium containing 20% fetal calf serum.

Cells were then suspended (10^5/ml) in culture medium supplemented with 200 μg/ml endothelial growth supplement (bovine pitu-

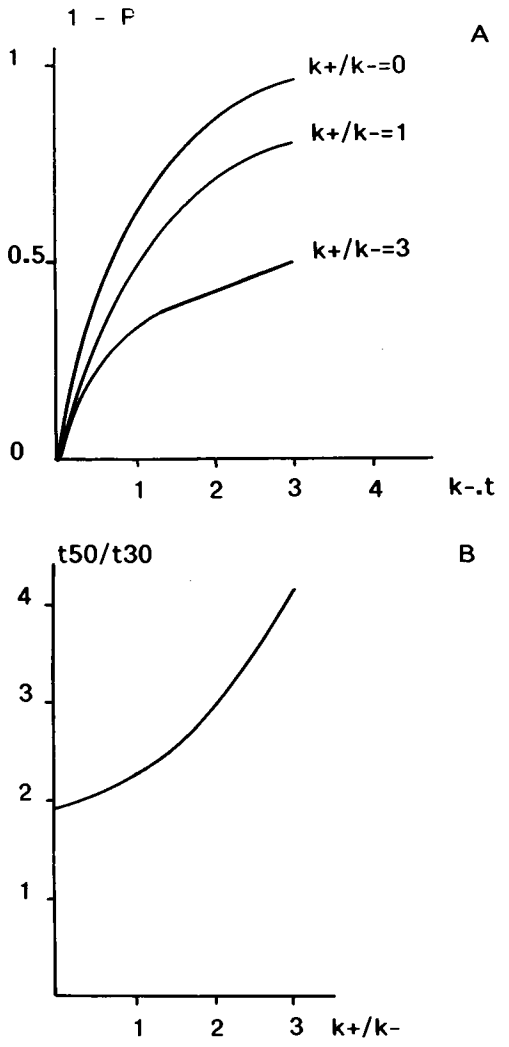

FIGURE 2 Minimal model of cell adhesion. The probability P that a cell remains bound by at least one bond until time t after the formation of the first bond was calculated with different values of bond formation and dissociation rates k_+ and k_-. (A) Three representative plots of ($1 - P$) vs. dimensionless product $k_- \cdot t$ are shown. (B) These curves were used to calculate the ratio t_{50}/t_{30} between times when 50 and 30%, respectively, of initially arrested cells had resumed their movement; this ratio was plotted vs. k_+/k_- in order to allow numerical derivation of k_+/k_- from experimental distributions of arrest durations.

itary EGS, Sigma) and deposited on 10×20-mm^2 glass coverslips that had been incubated overnight in 1% gelatin solution. Medium was changed every 48 h until confluency was obtained.

Before each experiment, cells were incubated for 4 h at 37°C with 10 U/ml of recombinant interleukin 1 (supplied by Tebu, Genzyme, Le Perray en Yveline, France). They were then washed and incubated for 0.5 h in normal medium before adhesion assay. It was checked microscopically that they displayed typical cobblestone appearance and they expressed von Willebrand antigen.

Human polymorphonuclear leukocytes were prepared with blood drawn from healthy volunteers in heparinized tubes (31). Briefly, cells were centrifuged on a barrier of high density Ficoll-containing medium (MSL, Eurobio, France). Pelleted granulocytes were then separated from contaminating erythrocytes by 1-g sedimentation for 20 min in 1.5% dextran solution (500,000 mol/wt, Pharmacia, Uppsala, Sweden). Finally, remaining erythrocytes were lysed by hypotonic shock (30 s). Activation was achieved by exposing cells for 5 min to 10^{-7} M *N*-formyl methionyl-leucyl-phenylalanine (FMLP, Calbiochem, supplied by France-biochem, Meudon, France). They were then used immediately.

Inhibition of adhesion

Mouse anti-E-selectin monoclonal antibody (anti-ELAM-1; reference BBA2) was supplied by British Bio-technology (Oxon, UK). Adhesion blockade was performed by incubating HUVECs with 50 μg/ml anti-ELAM-1 antibody for 30 min at room temperature immediately before binding assay.

Flow chamber

We used an apparatus that was described in previous reports (26, 29). A rectangular cavity ($17 \times 6 \times 1$ mm^3) was cut into a Plexiglas block ($20 \times 12 \times 45$ mm^3). The bottom wall of the chamber was a 22×10.5-mm^2 glass coverslip (170-μm thickness) coated with endothelial monolayers. It was stuck with silicon glue (Rubson, Brussels, Belgium). The flow was generated with a plastic syringe (2 ml) mounted on an electric syringe holder (Razel Scientific, supplied by Bioblock, France) equipped with a 2-rpm asynchronous electric motor.

Microscopic observation and image analysis

The chamber was set on the stage of an inverted microscope (model IM; Olympus, Tokyo, Japan) equipped with a videocamera (model 4015; Lhesa, Cergy Pointoise, France). Studies were done with a ×40 dry objective. All data were recorded with a tape recorder (model HS338; OSI, Paris, France) for delayed study.

Cell movement was studied with image analysis equipment that was previously described (32). The video signal was processed by a real-time digitizer (PcVision+, Imaging Technology, Woburn, MA) mounted on an IBM-compatible desk computer. This provided 512×512 pixel images with 256 gray levels. The final resolution was 0.42 μm per pixel. Digitized images were displayed on a screen monitor after reverse digital/analog conversion. A cursor driven by the computer mouse was superimposed on the image. Two methods were used to follow cell movements.

(a) The simplest method (method A) was to superimpose manually the cursor on the cell center and record its coordinates with the computer. This procedure was followed in all cases except accurate determination of arrest duration. A total number of 427 individual cells and 10,461 positions were used for data processing.

(b) To improve the accuracy of time and position determinations, the following procedure was used (method B): moving cells were followed by the cursor, and the computer continuously transferred small (32×32-pixel) images from digitizer to host computer random access memory. It appeared convenient to record five such images per second. A total of 256 images could be stored in a 256-kB zone of computer memory before transfer to mass storage (hard disk) for delayed analysis. Images were then subjected to individual examination for accurate (one-pixel accuracy) determination of the cell boundary. Indeed, no automatic algorithm was found suitable to determine cell boundaries with sufficient reliability. A total number of 119 cells (~5,000 individual images) were studied.

All operations were performed with laboratory-written software. Time determinations were done with the computer clock, with 0.01-s accuracy. Hence, the main limitation of velocity determinations was errors of position measurement.

Check of the flow

The flow was checked by monitoring a suspension of latex beads of 0.8-μm diam (Sigma Chemical) and focusing the microscope at various distances from the chamber floor for measuring bead velocity.

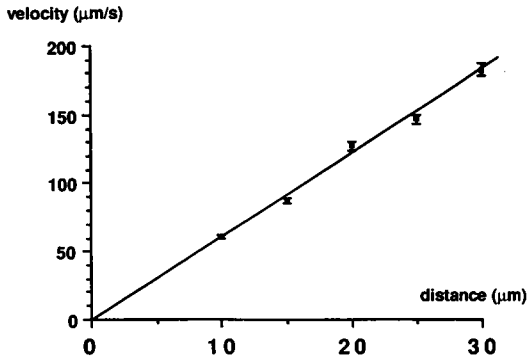

FIGURE 3 Calibration of the flow. The flow was calibrated by studying the velocity of small-diameter latex beads at different distances from the chamber floor. Each point is a mean of 10 separate measurements. Vertical bar length is twice the standard error.

Indeed, only the beads that were within 1–2 μm from the focus plane were visible (33).

Data analysis

Six series of experiments were performed, and results were pooled for statistical analysis.

Occurrence frequencies were compared after calculating theoretical standard errors as prescribed by Snedecor and Cochran (34).

The frequency of cell arrests was quantitatively estimated as previously described (35) by defining as $p \cdot dx$ the probability that a cell would become bound on the substrate after moving along a path of infinitesimal length dx. The a priori probability P that a cell entering the monitor screen moved along a pass L without any arrest before exit was thus given by

$$P = \exp(-p \cdot L). \qquad (11)$$

Conversely, the probability that an observed cell stopped after rolling along a path of length L was proportional to $p \cdot \exp(-p \cdot L)$. The a priori probability of observing a population of N cells with L_T total path length and n first stops was therefore equal to $p^n \cdot \exp(-p \cdot L_T)$. Parameter p was thus derived from experimental values of n and L_T by maximizing the above expression, which yielded the very simple formula

$$p = n/L_T, \qquad (12)$$

where n is the number of cell stops and L_T is the sum of the lengths of the individual cell trajectories.

RESULTS

Flow was laminar with constant velocity near the chamber floor

First, we verified that the flow was laminar by measuring the velocities of latex beads at different distances from the chamber floor. As shown on Fig. 3, the fluid velocity v at any point M separated from the chamber floor by a distance z was proportional to z with gradient velocity G equal to 5.25 s^{-1}:

$$v = G \cdot z.$$

We checked that G was effectively constant in all observation areas.

Cell positions are determined with 1–2 μm accuracy with mouse-follow procedure

It was essential to check the accuracy of position measurements, since this set the limit of detection of short-term cell arrests. We tested the reproducibility of the determination of cell positions with mouse-driven cursor; the motion of a series of typical cells was analyzed 10 times by replaying the same sequence with the tape recorder. Cell positions were determined with 1–2 μm accuracy. This was found sufficient to detect significant cell arrests, since cell shape irregularities made difficult a substantial refinement of the measurement procedure. Also, the standard deviation obtained in a series of measurements of arrest duration was ~0.2 s. However, a more precise technique was used to obtain the distribution of durations of short-term cell arrests (see below).

Cells moving in contact with endothelial cells are easily discriminated from faster elements

Since we were interested primarily in the efficiency of leukocyte–endothelium adhesion, it was essential to take account only of moving cells that were in actual contact with endothelial monolayers. This discrimination was easily achieved by combining several criteria. First, leukocytes moving close to endothelial cells had rather sharp boundaries, whereas other cells appeared as blurred moving shapes (Fig. 4). Second, leukocyte–substratum interaction resulted in marked irregularities of

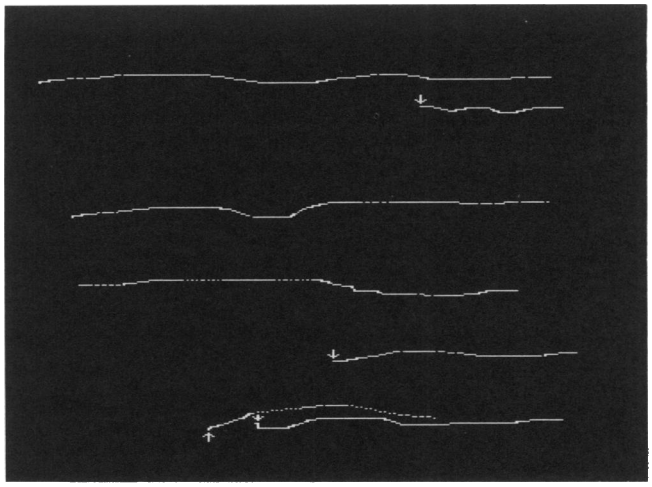

FIGURE 4 Detection of rolling leukocytes. The microscope was focused a few micrometers above the endothelial cell monolayers before driving leukocyte suspensions with calibrated shear flow. Rolling leukocytes (*arrow*) were discriminated from cells more distant from the chamber floor (*double arrow*) since the former were characterized by (*a*) lower velocity, (*b*) sharper boundaries, (*c*) visible rotation as detected by observing the motion of surface irregularities, and (*d*) marked irregularities of both direction and velocity. Horizontal bar is 12.5 μm.

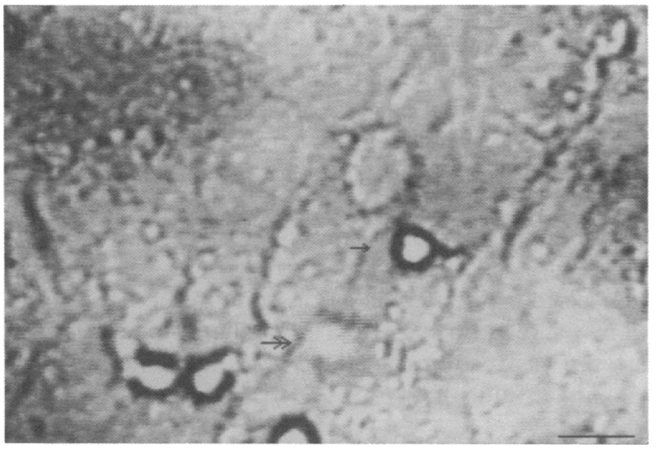

FIGURE 5 Typical trajectories of rolling granulocytes. The trajectories of seven typical leukocytes are shown. They displayed marked turns caused by their interaction with endothelial cells. Four of them are interrupted, revealing cell-to-substrate binding (*arrows*).

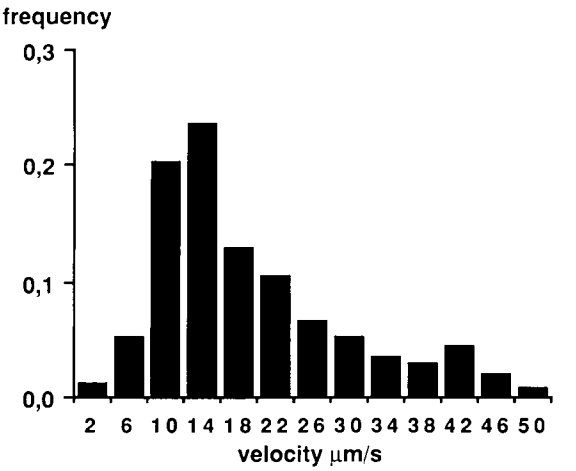

FIGURE 7 Velocity distribution of rolling leukocytes. Individual rolling leukocytes were followed along paths of 100–200 μm each for determination of their mean velocity. The velocity distribution of a sample of 363 cells is shown.

the motion, including both curvature of trajectories (Fig. 5) and temporal variations of the leukocyte velocity (Fig. 6), with transient or durable arrests that will be described below. On the contrary, cells that were at distance from the monolayer followed straight lines. Finally, leukocytes interacting with endothelium exhibited definite rolling, as evidenced by the motion of visible cell surface asperities.

Marked differences are found between the rolling velocities of different cells

The velocity distribution of 363 individual cells is shown on Fig. 7: important variations were found, since measured velocities ranged between ~2 and 50 μm/s. These differences could not be ascribed to size heterogeneity since in a sample of 42 cells (mean radius: 4.0 ± 3.2 μm [SD]) the mean ratio between velocity U and radius a was 2.9 s^{-1} (SD = 1.4, range 1.4–7.45) and the correlation coefficient between radius and velocity was −0.039, which was not significantly different from zero. Also, the velocity of a given cell remained fairly constant when it rolled across the observation field, apart from arrests described below.

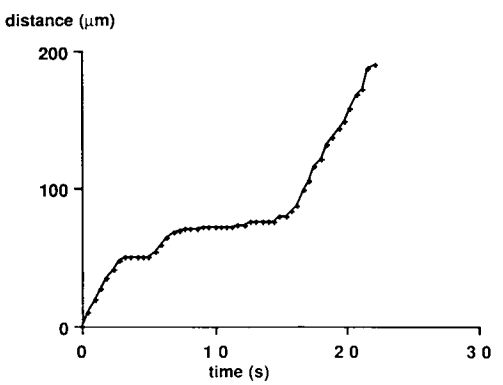

FIGURE 6 Motion of a typical cell. A granulocyte rolling along the endothelial cell monolayer was followed and sequential values of distance to the edge of the microscopic field (*ordinate*) were plotted vs. time. Sequences of movement with fairly constant velocity are separated by short-term binding events.

Cells exhibit frequent arrests of highly heterogeneous duration

As exemplified on Fig. 6, cell motion exhibited marked slowing events, with >10-fold reduction of translation velocity. To study these events, we needed operational definitions of "cell arrest." Three different procedures were used.

The simplest procedure was to count the cells rolling across the same microscopic field during a run (standard duration: 5–6 min) and determine the number of bound cells at the end of the flow. A typical field is shown on Fig. 8. During the six series of experiments described in this report, a total of 402 cells were counted and 129 of them remained bound. The mean fraction of durably attached cells was thus equal to 0.32. Also, after each run, the whole monolayer was scanned microscopically to check that the field selected for measurements was representative of other regions.

The second procedure was based on cell-follow with computer mouse-driven cursor (method A). On view of the accuracy of the measurement procedure, it appeared convenient to consider a cell as arrested when it had not moved by >2.4 μm (i.e., six pixels) during three sequential measurements (thus spanning a period of ~0.9 s). Out of 167 cells that were followed, 62 displayed at least one arrest, which represented a fraction of 0.37. The ad-

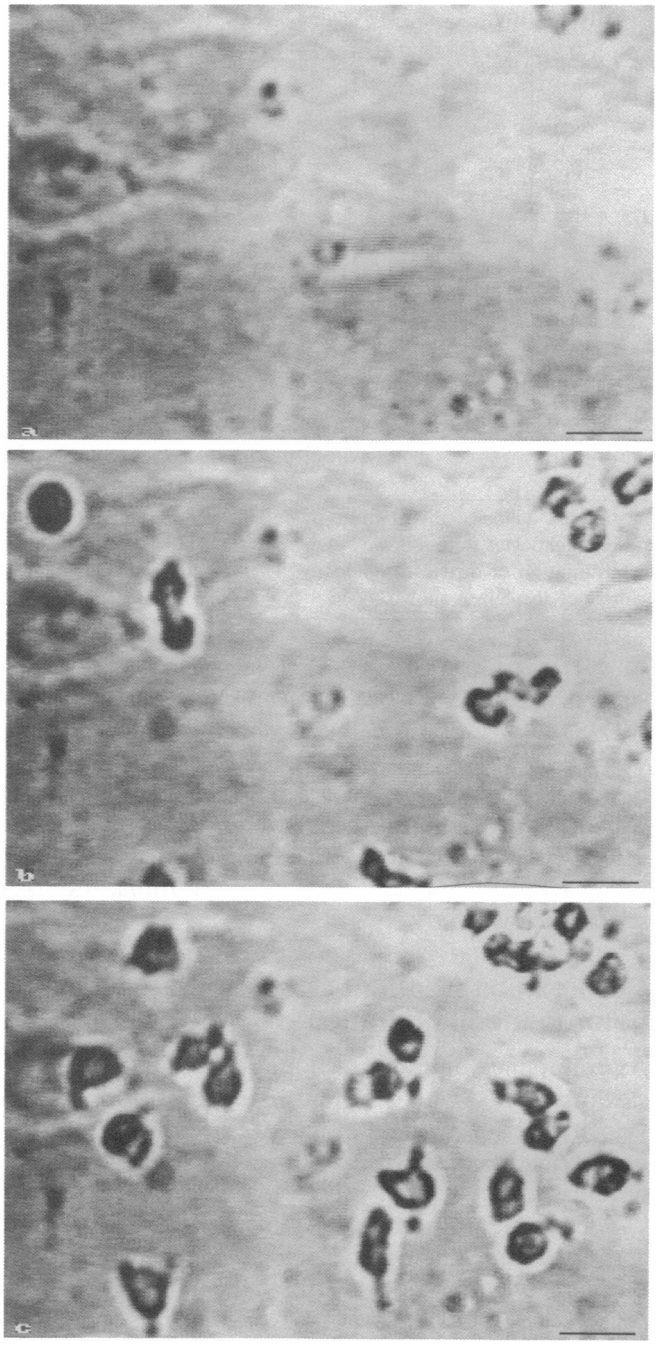

FIGURE 8 Long-term adhesion. Granulocytes were driven along endothelial cells for periods of 5 min with continuous observation of a fixed microscope field. The image processing system allowed rapid (a few seconds) transfer of field images to the computer memory. It was thus possible to record the time of arrest and departure of individual cells exhibiting binding events. Leukocytes rolling across the field were counted. The field aspect is shown before (*a*), during (*b*), and after (*c*) leukocyte passage. Horizontal bar length is 10 μm.

hesion probability parameter was $p = 0.00206\ \mu m^{-1}$, corresponding to a stop every 485 μm. Taken at face value, these figures would suggest that nearly all cell arrests resulted in durable (i.e., several minutes') attachment. This possibility was tested by studying the distribution of cell arrest duration with a more refined method. Thus 97 individual cells were followed by continuous recording of local images and delayed analysis of cell position (method B). A typical set of images is shown on Fig. 9. The sampling frequency was about five images per second and >5,000 positions were recorded. A cell was considered as arrested if it moved by <0.8 μm during a 0.4-s period of time. 67 cells (i.e., 69%) displayed at least one transient arrest during the observation period. The frequency distribution of arrest duration is shown on Fig. 10. The median duration of cell arrests was readily calculated by linear interpolation, yielding a value of

$$T_{50} = 2.43\ s;$$

similarly, 30% of arrested cells resumed their movements after a stay of duration t_{30} equal to 0.97 s. Using Fig. 2 *B*, the corresponding value of the ratio k_+/k_- defined in our simple model was 1.5. As shown on Fig. 10, the agreement between experimental points and the theoretical curve calculated with this value was quite satisfactory. The corresponding values of parameters k_+ and k_- were 0.75 and 0.50 s^{-1}, respectively. It was not surprising to find that k_+ was much larger than the product between p and cell velocity (i.e., $\sim$0.03 s^{-1}), since the cell–substrate distance was probably not optimal for bond formation when cells were freely moving.

Furthermore, we monitored the motion of cells resuming their movement after a brief stop. Nearly 91% of these cells exhibited a second arrest before rolling out of the microscope field, yielding an adhesion probability parameter of 0.041 μm^{-1} for the second stop. This was

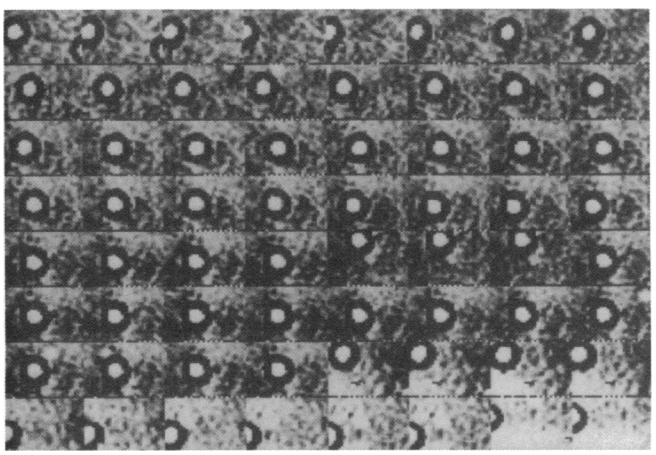

FIGURE 9 Determination of cell position by continuous image transfer. Rolling leukocytes were followed with a cursor driven by the computer mouse. This allowed continuous and rapid (0.2 s) transfer of 32 × 32-pixel images containing a given cell. This permitted easy derivation of the exact (1-pixel accuracy) cell position from its position within each image together with recorded image position. A typical series of images is shown. Each one represents an area of $\sim 27 \times 27\ \mu m^2$.

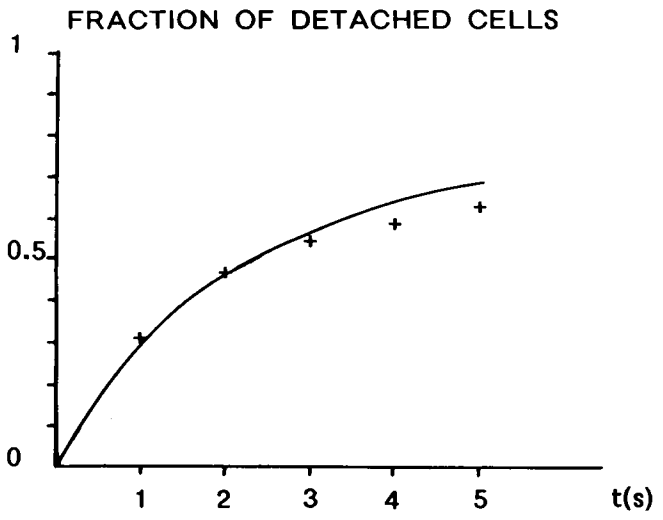

FIGURE 10 Duration of individual cell arrest. 150 cells exhibiting transient or durable arrest were followed for determination of arrest duration. The fraction of arrests lasting more than 1, 3, 3, 4, or 5 s are shown together with a fitted curve obtained with the model described in Fig. 2 by fitting the values of t when 30 and 50% of cells resumed their movement.

not due to a decreased rolling velocity (see Fig. 11); indeed, in a sample of 21 cells exhibiting two arrests or more, the mean velocity was 8.9 μm/s (SD = 3) and 6.4 μm/s (SD = 3.2) before the first arrest and between the first and second arrests, respectively. The mean path lengths before the first and second arrests were 43.7 and 13.1 μm, respectively.

Since 32% of cells exhibited durable attachment, and 37% exhibited at least one arrest detectable with method A, our data strongly support the overall conclusion that most cells exhibiting a detectable arrest, whatever its length, eventually remained firmly adherent to endothelial cells for several minutes or more. This supports the biological significance of detected arrests.

Cell stop does not require progressive slowdown, but arrest frequency is higher when cell rolling velocity is low

It was of interest to know whether cell arrest was usually preceded by a gradual decrease of translational velocity. 66 cell arrest events were thus studied for determination of the mean cell velocity (a) during the 5–10 s before arrest (V_1), (b) during the last second before arrest (V_2), and (c) during the last fifth of a second before arrest (V_3). The mean values of parameters V_2 and V_3 were, respectively, 90% (±2.6% SE) and 89% (±4.9% SE) of V_1. Thus, no substantial slowdown was detected before cell arrest, in accordance with the hypothesis that arrest was mediated by a single molecular bond.

However, as shown on Fig. 11, there was a sharp negative correlation between the mean velocity of rolling leukocytes and the probability that they display at least one stop during the period of observation. Indeed, out of 383 individual cells, 81% of those rolling slower than 8 μm/s displayed at least one arrest whereas only 25% of those rolling faster than 16 μm/s stopped. It is concluded that the surface parameters determining cell rolling velocity play a critical role in the binding process under flow conditions.

Pretreating endothelial cells with anti-E-selectin inhibits leukocyte–endothelium attachment

It was important to know whether the adhesive events demonstrated under our dynamic conditions were dependent on the cell structures and functions previously shown to play a role in granulocyte adhesion. For this

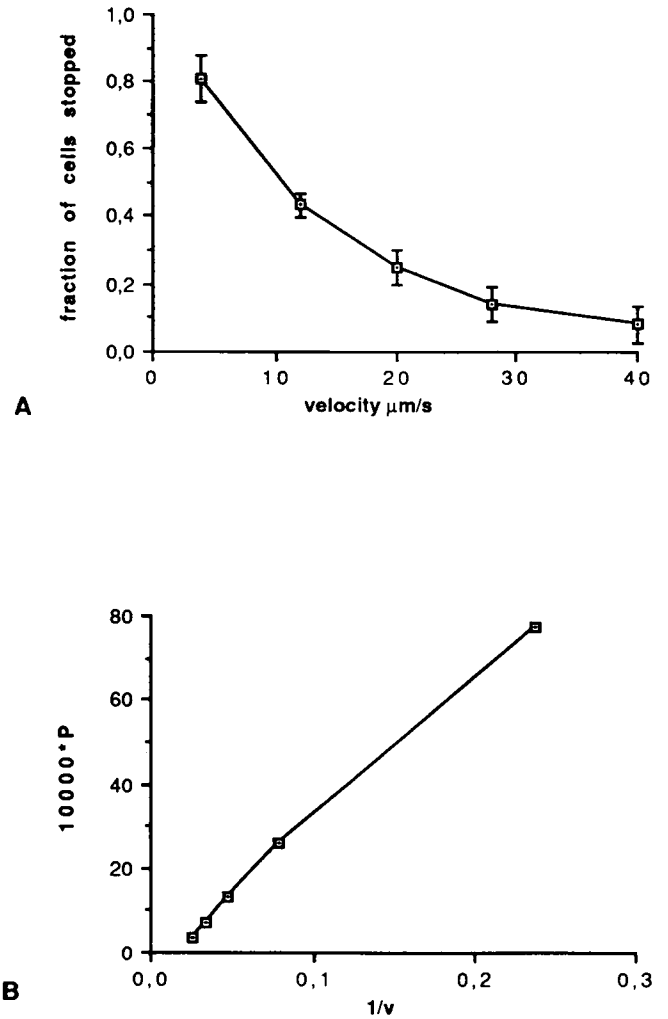

FIGURE 11 Dependence of binding frequency on rolling velocity. The velocities of 383 individual granulocytes were measured. They were separated in five velocity classes, and the proportion of cells displaying at least one arrest during their passage across the microscope field was calculated. Results are shown together with expected standard error (A). The binding efficiency parameter p was calculated as explained (using Eq. 11) and plotted vs. the reciprocal value of cell velocity (B).

purpose, we used anti-E-selectin antibodies to inhibit granulocyte arrest. As shown in Table 2, the treatment of endothelial cells significantly ($P < 0.005$) inhibited long-term adhesions (as determined by counting bound cells after a 5-min flow). A more detailed study of the effect of this treatment showed that the antibody decreased the fraction of cells exhibiting at least one arrest ($P = 0.017$) rather than arrest duration (Table 3).

Anti-E-selectin did not affect rolling velocity under our experimental conditions

Since binding probability was negatively correlated to cell rolling velocity (Fig. 11), it was of obvious interest to determine whether anti-E-selectin treatment inhibited cell binding by increasing translational velocity. The mean velocity of rolling cells was thus determined under various experimental conditions. Mean values were 19.0 ± 9.7 (SD) μm/s ($n = 162$ cells) and 16.0 ± 7.9 (SD) μm/s ($n = 91$) for controls and antibody-treated samples, respectively. Thus, anti-E-selectin did not increase rolling velocity under our experimental conditions.

DISCUSSION

We described the translational motion of human granulocytes rolling along endothelial cells in presence of a hydrodynamic drag force ~10-fold weaker than a standard ligand–receptor bond. We observed repeated cell arrests with a median duration of 2.43 s. The frequency, not the length, of these arrests was significantly inhibited by anti-E-selectin antibodies.

The hypothesis that the arrests we observed were caused by single ligand–receptor bonds is supported by the following points.

(*a*) Cell arrest was not preceded by a progressive slowdown, which would be suggestive of a progressive increase of bond number.

(*b*) The finding that anti-E-selectin antibodies reduced stop frequency, not duration, strongly suggests that (*a*) associations between E-selectin and granulocyte counterreceptor were responsible for at least part of arrests, and (*b*) when a cell had stopped, additional E-selectins were not involved in bond strengthening. It is therefore reasonable to assume that single selectin–receptor bonds might be responsible for a substantial proportion of observed arrests. It may be added that, although interactions between leukocyte integrins and endothelium ICAM might in principle contribute cell–substratum adhesion (9), integrin activation and ICAM expression were not optimal under our experimental conditions. However, some ICAM-mediated bonds might be involved in the bond strengthening responsible for the longer duration of a proportion of cell arrests.

(*c*) The distribution of arrest durations was consistent with the predictions of a minimal model of bond formation and dissociation (Fig. 10). The best fit for bond formation and dissociation rates were 0.75 and 0.5 s^{-1}, respectively. Using these parameters, a numerical simulation yielded ~2.0 for the mean number of bonds between a cell and the substratum after 6-s arrest. This result suggested that most observed short-term cell–substratum adhesions were mediated by one or two bonds.

Now, several important issues may be discussed in view of our experimental results.

TABLE 2 Effect of anti-E-selectin on durable attachment of granulocytes to endothelial cells under flow conditions

Inhibitor used	Number of:		Fraction of bound cells
	Rolling cells	Bound cells	
None	402	129	0.32 ± 0.023
Anti-E-selectin	224	21	0.09 ± 0.019

In six series of experiments, blood granulocytes were made to roll on endothelial cell monolayers during runs of ~5-min duration. The number of rolling cells was recorded as well as the number of cells remaining bound after each run. The fraction of bound cells was determined under control or inhibitory conditions. Theoretical standard errors were calculated following Snedecor and Cochran (34). Anti-E-selectin significantly inhibited binding ($P < 0.000001$).

TABLE 3 Effect of anti-E-selectin on the frequency and duration of leukocyte arrest on endothelial cell monolayers

Inhibitor used	Cell number	Counted cells with at least one arrest		Number of cells with first arrest >2 s	
		Number	Percent	Number	Percent
None	167	62	37 ± 4	38/62	61 ± 6
Anti-E-Selectin	100	23	23 ± 4	17/23	74 ± 9

Individual rolling leukocytes were monitored to determine (*a*) the proportion of cells exhibiting at least one stop during their passage through the microscope field and (*b*) the proportion of first arrests with duration higher than 2 s. Standard errors are shown as calculated following Snedecor and Cochran (34). The antibody treatment reduced the frequency of overall arrests ($P = 0.017$), without reducing their mean duration.

Is the estimated bond lifetime consistent with currently available data?

In a recent report, Moore et al. (36) studied the interaction between granulocytes and P-selectin, a molecule closely related to E-selectin and with a similar specificity (37). The binding of P-selectin was reversible and saturable, with a maximum of 20,000 sites per leukocyte, and half-maximum equilibrium binding at a free ligand concentration of 1.5 nM. Furthermore, a kinetic study (see Fig. 1 or reference 36) revealed that ~240 s was required for half completion of binding at 0.1 nM ligand concentration. As derived by standard equations of reaction ki-

netics (Appendix), the spontaneous rate of ligand separation from cell binding sites toward bulk medium (i.e., parameter k_-) is $\sim 0.0027\ s^{-1}$. Furthermore, as clearly argued by Bell (17), assuming that the binding reaction we consider is diffusion limited, the dissociation rate of complexes made between membrane-bound ligands is expected to be nearly 10,000-fold lower than for free molecules. Hence, the natural lifetime of a single bond between membrane-bound selectins and counterreceptors (i.e., $\sim 10{,}000/0.0027$ s) is quite sufficient to account for the observed duration of cell arrest. Indeed, these arrests are about one million times shorter than expected!

The simplest explanation for this discrepancy is that the hydrodynamic drag force drastically reduced the lifetime of cell-to-substratum bonds. This does not seem consistent with Bell's estimate (17) based on Zurkhov's report (18) on the fracture of material samples. However, it is quite reasonable to expect the behavior of single bonds to be quite different from that of macroscopic materials. Clearly, a study of the effects of stress on individual bonds would be useful to understand the mechanisms of adhesion rupture. A study of the influence of the shear rate on cell arrest duration under our experimental conditions would be useful in this respect.

Absolute rate of bond formation between endothelial cells and rolling granulocytes is on the order of 0.04 s^{-1}

The empirical binding parameter p derived from the average stop frequency was $0.002\ \mu m^{-1}$. The corresponding rate of bond formation may be readily derived by multiplying this value by the average leukocyte rolling velocity (i.e., 19 μm/s), yielding an estimate of 0.038 s^{-1}. About 10-fold higher rates of bond formation were obtained with (*a*) substratum-bound cells: parameter k_+ was $0.75\ s^{-1}$, and (*b*) cells resuming their movement after a brief stop. These differences are consistent with the hypothesis that bond formation may be easier before and immediately after cell stop because of a suitable reorganization of repeller elements present in the cell coat (15, 16, 38). This reorganization might involve time-dependent compression of polymeric molecules or diffusion out of contact areas. Also, formation of additional bonds on an arrested cell may be enhanced by hydrodynamic forces in some contacts (see double arrow, Fig. 2 *A*). Another important possibility would be that purely hydrodynamic forces impair cell-to-substrate approach. This is strongly supported by a study performed by Wattenbarger et al. (39), who reported on the adhesion of glycophorin-coated liposomes to a lectin surface in shear flow: although liposomes were obviously smooth, the width of the substrate–particle gap estimated with Goldman's equation was comparable to that obtained in this study. However, it must be noted that entropic repulsive forces might play a role in liposome adhesion (40). Admittedly, more direct observations are required to validate these hypotheses. Interestingly, the value obtained for the rate of bond formation is consistent, within an order of magnitude, with the maximum rate of bond formation derived by Bell for cell bearing ~ 250 ligand molecules/μm^2 and adhering via a contact area of $\sim 0.01\ \mu m^2$, corresponding to the tip of a microvillus.

Rate of bond formation is a slowly decreasing function of cell rolling velocity

As shown on Fig. 11, the stop frequency was inversely correlated to cell translation velocity. According to Eq. 11, the probability P that a cell went across the observation field without any stop was $\exp(-pL)$, where L is the width of the microscope field ($L = 215\ \mu m$). As shown on Fig. 11 *B*, parameter p was fairly proportional to $1/U$, where U is the cell translation velocity. Indeed, the product pU exhibited about a twofold decrease when U increased by a factor of nine (Fig. 11).

Parameters determining cell translation velocity under our experimental conditions deserve further study

Whereas it seems well demonstrated that selectin-mediated interactions are responsible for the rolling phenomenon observed at high shear rate (i.e., $G > 100\ s^{-1}$, see reference 9), under our experimental conditions, these interactions were responsible for the visible stops we observed. However, they did not influence rolling velocity, as demonstrated by the lack of effect on anti-E-selectin antibodies on this parameter. It is therefore important to know the reason for the high individual variations of rolling velocities (Fig. 9). These were not due to cell size differences, inasmuch as cell diameter and velocity were not correlated. Also, they were not due to irregularities of the hydrodynamic flow, due to thickness variations of the endothelial monolayer, since the velocity of individual cells was fairly constant during their passage through the entire microscope field. More work is required to determine whether these irregularities are due to molecular interactions between granulocytes and endothelial cells, which might be expected in view of the extensive simulations performed by Hammer and Apte (22), or this is dependent on hydrodynamic effects in absence of any actual molecular bonding (39). Also, the possibility of molecular interactions weaker than ligand–receptor bonds might be considered in view of previous experimental evidence (26).

In conclusion, our experimental approach allowed fairly direct observation of the kinetics of bond formation and rupture between formyl-peptide–stimulated human granulocytes and interleukin-1–activated human endothelial cells. Bonds involving E-selectin were found to play a role in this interaction, and numerical

values were obtained for the rate of bond formation and dissociation.

APPENDIX

Let us consider the kinetics of binding of soluble ligand molecules L to membrane-bound binding sites S:

$$L + S \underset{k^-}{\overset{k^+}{\rightleftharpoons}} LS.$$

Let α be the fraction of bound sites {i.e., $\alpha = (SL)/[(S) + (SL)]$}. Using standard theory of reaction kinetics, we may write

$$d\alpha/dt = k^+(1 - \alpha)(So)(L) - k^-\alpha(So),$$

where (So) represents the sum of free and ligand-bound membrane sites. The above equation is notably simplified if it is assumed that the amount of ligand molecules is much higher than the number of binding sites. (L) may then be considered as constant and the above equation is readily integrated, which yields

$$\alpha = (1 - \exp\{-[k^- + k^+(L)]t\})k^+(L)/[k^- + k^+(L)],$$

where it is assumed that free ligand is added at time zero. Now, defining at $(L_{1/2})$ the ligand concentration yielding 50% of bound sites when equilibrium is reached, and $t_{1/2}$ the time required to achieve 50% of equilibrium binding when the ligand concentration is L, we obtain

$$(L_{1/2}) = k^-/k^+$$
$$t_{1/2} = \ln 2/[k^- + k^+(L)].$$

These equations were used to extract k^+ and k^- from experimental data reported by Moore et al. (36).

The authors are indebted to Dr. Valette and his technical staff at St. Joseph Hospital for providing umbilical cords.

This work was supported by grant CJF 8907 from the Instiut National de la Sante et de la Recherche Medicale and by the Assistance Publique de Marseille.

Received for publication 25 November 1992 and in final form 16 February 1993.

REFERENCES

1. Rothstein, T. L., M. Mage, G. Jones, and L. L. McHugh. 1978. Cytotoxic T lymphocyte sequential killing of immobilized allogeneic tumor target cells measured by time-lapse microcinematography. *J. Immunol.* 121:1652–1656.
2. Lee, D. A., J. R. Hordal, D. J. Garlich, C. C. Clawson, P. G. Quie, and P. K. Peterson. 1984. Opsonin-independent phagocytosis of surface-adherent bacteria by human alveolar macrophages. *J. Leukocyte Biol.* 36:689–701.
3. Zhu, D. Z., C. F. Cheng, and B. U. Pauli. 1991. Mediation of lung metastasis of murine melanomas by a lung-specific endothelial cell adhesion molecule. *Proc. Natl. Acad. Sci. USA.* 88:9568–9572.
4. Gould, K., C. H. Ramirez-Ronda, R. K. Holmes, and J. P. Sanford. 1975. Adherence of bacteria to heart valves in vitro. *J. Clin. Invest.* 56:1364–1370.
5. Harlan, J. M. 1985. Leukocyte-endothelial cell interaction. *Blood.* 65:513–525.
6. Bevilacqua, M. P., J. S. Pober, M. E. Wheeler, R. S. Cotran, and M. A. Gimbrone. 1985. Interleukin-1 acts on cultured human vascular endothelium to increase the adhesion of polymorphonuclear leukocytes, monocytes and related leukocyte cell lines. *J. Clin. Invest.* 76:2003–2011.
7. Springer, T. A. 1990. Adhesion receptors of the immune system. *Nature (Lond.).* 346:425–434.
8. Atherton, A., and G. V. R. Born. 1972. Quantitative investigations on the adhesiveness of circulating polymorphonuclear leukocytes to blood vessel walls. *J. Physiol. (Lond.).* 222:447–474.
9. Lawrence, M. B., and T. A. Springer. 1991. Leukocytes roll on a selectin at physiological flow rates: distinction from and prerequisite for adhesion through integrins. *Cell.* 65:859–873.
10. Detmers, P. A., S. D. Wright, E. Olsen, B. Kimball, and Z. A. Cohn. 1987. Aggregation of complement receptors on human neutrophils in the absence of ligand. *J. Cell Biol.* 105:1137–1145.
11. Dustin, M. L., and T. A. Springer. 1989. T-cell receptor cross-linking transiently stimulates adhesiveness through LFA-1. *Nature (Lond.).* 341:619–624.
12. Kuipjers, T. W., B. C. Hakkert, M. H. C. Hart, and D. Roos. 1992. Neutrophil migration across monolayers of cytokine-stimulated endothelial cells: a role for platelet-activating factor and IL-8. *J. Cell Biol.* 117:565–572.
13. Bongrand, P., and G. I. Bell. 1984. Cell-cell adhesion: parameters and possible mechanisms. *In* Cell Surface Dynamics: Concepts and Models. A. S. Perelson, C. DeLisi, and F. W. Wiegell, editors. Marcel Dekker Inc., New York. 459–493.
14. Bongrand, P., editor. 1988. Physical Basis of Cell-Cell Adhesion. CRC Press, Boca Raton, FL. 267 pp.
15. André, P., and P. Bongrand. 1990. *In* Cell–Cell Contacts. R. Glaser and D. Gingell, editors. Springer Verlag, Berlin. 287–321.
16. Bongrand, P. 1993. Adhesion of cells. *In* Structure and Conformation of Membranes. R. Lipowsky, editor. Springer Verlag, Berlin. In press.
17. Bell, G. I. 1978. Models for the specific adhesion of cells to cells. *Science (Wash. DC).* 200:618–627.
18. Zurkhov, S. N. 1965. Energetic concept of the strength of solids. *Int. J. Fract. Mech.* 1:311–323.
19. Hammer, D. A., and D. A. Lauffenburger. 1987. A dynamical model for receptor-mediated cell adhesion to surfaces. *Biophys. J.* 52:475–487.
20. Dembo, M., D. C. Torney, K. Saxman, and D. Hammer. 1988. The reaction-limited kinetics of membrane-to-surface adhesion and detachment. *Proc. R. Soc. Lond. B. Biol. Sci.* 234:55–83.
21. Cozens-Roberts, C., D. A. Lauffenburger, and J. A. Quinn. 1990. Receptor-mediated cell attachment and detachment kinetics. I. Probabilistic model and analysis. *Biophys. J.* 58:841–856.
22. Hammer, D. A., and S. M. Apte. 1992. Simulation of cell rolling and adhesion on surfaces in shear flow: general results and analysis of selectin-mediated neutrophil adhesion. *Biophys. J.* 63:35–57.
23. Tözeren, A., and K. Ley. 1992. How do selectins mediate leukocyte rolling in venules? *Biophys. J.* 63:700–709.
24. Lauffenburger, D. A., and Linderman, J. J. 1993. Receptors: Models for Binding, Trafficking and Signalling and Their Relationship to Cell Function. Oxford University Press, London. In press.
25. Goldman, A. J., R. G. Cox, and H. Brenner. 1967. Slow viscous motion of a sphere parallel to a plane wall. II. Couette flow. *Chem. Engn. Sci.* 22:653–660.

26. Tissot, O., A. Pierres, C. Foa, M. Delaage, and P. Bongrand. 1992. Motion of cells sedimenting on a solid surface in a laminar shear flow. *Biophys. J.* 61:204–215.

27. Tha, S. P., J. Shuster, and H. L. Goldsmith. 1986. Interaction forces between red cells agglutinated by antibody. II. Measurement of hydrodynamic force of breakup. *Biophys. J.* 50:1117–1126.

28. Evans, E., D. Berk, and A. Leung. 1991. Detachment of agglutinin-bonded red blood cells. I. Forces to rupture molecular point attachments. *Biophys. J.* 59:838–848.

29. Tissot, O., C. Foa, C. Capo, H. Brailly, M. Delaage, and P. Bongrand. 1991. Influence of adhesive bonds and surface rugosity on the interaction between rat thymocytes and flat surfaces under laminar shear flow. *J. Dispersion Sci. Technol.* 12:145–160.

30. Gimbrone, M. A. 1976. Culture of vascular endothelium. *Prog. Hemostasis Thromb.* 3:1–28.

31. Mège, J. L., J. Pouget, C. Capo, P. André, A. M. Benoliel, G. Serratrice, and P. Bongrand. 1988. Myotonic distrophy: defective oxidative burst of polymorphonuclear leukocytes. *J. Leukocyte Biol.* 44:180–186.

32. André, P., J. Gabert, A. M. Benoliel, C. Capo, C. Boyer, A. M. Schmitt-Verhulst, B. Malissen, and P. Bongrand. 1991. Wild-type and tailless CD8 display similar interaction with microfilaments during capping. *J. Cell Sci.* 100:329–337.

33. Mège, J. L., C. Capo, A. M. Benoliel, C. Foa, and P. Bongrand. 1985. Study of cell deformability by a simple method. *J. Immunol. Methods.* 82:3–15.

34. Snedecor, G. W., and W. G. Cochran. 1980. *In* Statistical Methods. Iowa State University Press, Ames. 124–128.

35. Mège, J. L., C. Capo, A. M. Benoliel, and P. Bongrand. 1986. Determination of binding strength and kinetics of binding initiation. A model study made on the adhesive properties of P388D1 macrophage-like cells. *Cell Biophys.* 8:141–160.

36. Moore, K. K., A. Varki, and R. P. McEver. 1991. GMP 140 binds to a glycoprotein receptor on human neutrophils: evidence for a lectin-like interaction. *J. Cell Biol.* 112:491–499.

37. Foxall, C., S. R. Watson, D. Dowbenko, C. Fennie, L. A. Lasky, M. Kiso, A. Hasegawa, D. Asa, and B. K. Brandley. 1992. The three members of the selectin receptor family recognize a common carbohydrate epitope, the sialyl-Lewis oligosaccharide. *J. Cell Biol.* 117:895–902.

38. Bell, G. I., M. Dembo, and P. Bongrand. 1984. Cell adhesion: competition between nonspecific repulsion and specific bonding. *Biophys. J.* 45:1051–1064.

39. Wattenbarger, M. R., D. J. Graves, and D. A. Lauffenburger. 1990. Specific adhesion of glycophorin liposomes to a lectin surface in shear flow. *Biophys. J.* 57:765–777.

40. Hellfrich, W. 1978. Steric interaction of fluid membranes in multilayer systems. *Z. Naturforsch. Sect. A.* 33*a*:305–315.